Periostin promotes atrioventricular mesenchyme matrix invasion and remodeling mediated by integrin signaling through Rho/PI 3-kinase

Jonathan T. Butcher, Russell A. Norris, Stanley Hoffman, Corey H. Mjaatvedt, Roger R. Markwald *

Cardiovascular Developmental Biology Center, Chair of Cell Biology and Anatomy, Medical University of South Carolina, Basic Science Building Rm. 601, 173 Ashley Ave, Charleston, SC 29425, USA

Abstract

Recent evidence suggests that extracellular matrix components may play a signaling role in embryonic valve development. We have previously identified the spatiotemporal expression patterns of periostin in developing valves, but its function during this process is largely unknown. To evaluate the functional role periostin plays during valvulogenesis, two separate three-dimensional culture assay systems, which model chick atrioventricular cushion development, were employed. These assays demonstrated that cushion mesenchymal cells adhered and spread on purified periostin in a dose-responsive manner, similar to collagen I and fibronectin via $\alpha_v\beta_3$ and β_1 integrin pairs. Periostin overexpression resulted in enhanced mesenchyme invasion through 3D collagen gels and increased matrix compaction. This invasion was dependent on $\alpha_v\beta_3$ more than β_1 integrin signaling, and was mediated differentially by Rho kinase and PI 3-kinase. Both matrix invasion and compaction were associated with a colocalization of periostin and β_1 integrin expression to migratory cell phenotype in both surface and deep cells. The Rho/PI 3-kinase pathway also differentially mediated matrix compaction. Both Rho and PI 3-kinase were involved in normal cushion mesenchyme matrix compaction, but only PI 3-kinase was required for the enhanced matrix compaction due to periostin. Taken together, these results highlight periostin as a mediator of matrix remodeling by cushion mesenchyme towards a mature valve structure.
© 2006 Elsevier Inc. All rights reserved.

Introduction

Embryonic valve formation is a highly coordinated process involving a complex integration of cellular and matrix mediated processes. The initial loci for atrioventricular (AV) valve development are specific subsets of endocardial cells lining the primitive atrioventricular canal, which are adhered to a glycosaminoglycan rich matrix termed the "cardiac jelly" initially secreted by the underlying primary myocardium(Krug et al., 1985; Manasek et al., 1973). These myocardial cells directly subadjacent to the AV endocardial cells begin secreting growth factors, principally bone morphogenetic protein-2 (BMP-2) around Hamburger and Hamilton stage 14 (HH14) (Hamburger and Hamilton, 1992), which initiates a cascade of interrelated signal pathways resulting

in an endocardial transformation to mesenchyme (EMT). This is evidenced by the loss of expression of endocardial markers like VE-cadherin, CD31, and NCAM1, and gain of expression of mesenchymal markers such as α-smooth muscle actin (Person et al., 2005). These cells suspend their junctional contacts from neighboring endocardial cells and adopt an activated, migratory phenotype characterized by polarized cell bodies with numerous filamentous membrane extensions. These cells then invade the underlying matrix, secreting conditioning factors such as chondroitin sulfate and heparin sulfate, which both encourage additional mesenchymal invasion and synthesis of fibrillar proteins (Funderburg and Markwald, 1986). By HH25, the cardiac jelly has been remodeled into fully mesenchymalized swellings, dubbed "cushions", which eventually form the valves and septa of the mature 4-chambered heart. The morphogenesis of the AV valves from these cushions involve a process of proliferation, extension, condensation, and delamination (De la Cruz and Markwald, 2000). Beginning at HH26, by

---

a process not completely understood, a subendocardial zone of mesenchyme proliferates and migrates, extending the primitive tissue along an AV myocardial substrate (Oosthoek et al., 1998a). The portion of the cushion that interfaces with the myocardium begins to differentiate into a fibroblastic phenotype. This differentiated phenotype then begins to condense the cushion matrix into a thinner, more fibrous tissue. Fenestrations develop in the subadjacent myocardial layers by HH30 through an as yet unknown mechanism, which coalesce and delaminate the primitive leaflet from the myocardial walls. Residual connections to the myocardium are eventually remodeled into the tendinous chords and papillary muscles (De la Cruz and Markwald, 2000; de Lange et al., 2004; Oosthoek et al., 1998b). These processes are largely mediated by the maturing cushion mesenchyme, but the mechanisms behind this matrix remodeling process are largely unknown.

Recent evidence has identified several ECM components that are critical in regulating valvulogenesis. Camenisch et al. (2000, 2002) showed that hyaluronan synthase 2 (Has2) null mouse hearts failed to form cardiac jelly, which inhibited mesenchymal transformation (and ultimately absence of cardiac cushions) through impaired Ras signaling through ErbB2 receptors. The same result (no valves) was noted in hyaluronidase digested rat embryos (Baldwin et al., 1994) and UDP glucose-dehydrogenase (UGDH—an important enzyme in hyaluronic acid processing) deficient zebrafish (Walsh and Stainier, 2001). The proteoglycan versican, which binds collagen and hyaluronan, is also important for cushion formation as versican null mice also do not form cushions (Mjaatvedt et al., 1998). Endocardial transformation to mesenchyme is further characterized by the secretion of extracellular matrix molecules including collagens I, II, III, V, and VI, tenascin, aggrecan, and eventually elastin (Garcia-Martinez et al., 1991; Hurle et al., 1994; Lincoln et al., 2004). Each of these matrix components confers important spatiotemporal signals required for cushion remodeling and may be related to the aforementioned growth factor signaling networks. Lincoln et al. (2006a) determined that FGF stimulation of HH25 AV cushion mesenchyme resulted in the expression of tenascin, while BMP stimulation resulted in aggrecan expression. The effects of these constituents on cushion mesenchymal cells, however, remain to be determined.

We previously identified and characterized the spatiotemporal cardiac expression pattern of periostin, a secreted extracellular matrix protein belonging to the fasciclin gene family. During cardiac development, periostin expression is specifically localized to the subendocardial region of atrioventricular cushions and along the mesenchymal myocardial interface during the period of delamination (Kern et al., 2005; Kruzynska-Frejtag et al., 2001; Norris et al., 2004). This pattern of expression is very similar to the locations of the proliferation/remodeling zones in the AV cushions, suggesting that this ECM protein may play a role in mediating cushion remodeling (De la Cruz and Markwald, 2000).

The objective of this study therefore was to determine if periostin mediates the adhesion, invasion, and matrix condensation of Post-EMT AV cushion mesenchyme, and by what me-

chanism. To accomplish this, quantitative three-dimensional (3D) assays were developed to measure cell migration, invasion, and condensation independently over time. Data demonstrate that periostin enhances collagen invasion and condensation by cushion mesenchyme, potentially through specific integrin pairs and signal pathway cascades.

Materials and methods

Periostin structure and viral production

Periostin is an 811 amino acid polypeptide comprised of 4 repeating fasciclin domains (Fas1–4), an amino-terminal signal sequence (S.S.) and a putative glycosylation site in the 4th fasciclin domain (Litvin et al., 2005). A full-length mouse periostin clone (kind gift of Dr. Simon Conway, IUPUI) including the start site of translation and kozak sequence was cloned in the sense orientation into the pDNR adenoviral shuttle vector (Clontech). A chicken full-length cDNA clone (Norris et al., 2004) and a LacZ clone were also inserted into separate pDNR shuttle vectors (Supplemental Fig. 1). To make the chicken periostin anti-sense vector, the clone was inserted in reverse. Expression of all three transgenes was driven by the constitutively active cytomegalovirus (CMV) promoter. These clones were inserted directly into the Adeno-X genome through a cre-recombinase reaction, and screened for recombination. Positive recombinants were amplified in HEK293 cells and purified using an adenoviral purification kit (Clontech). To facilitate detection of virally produced periostin, a hemagglutinin (HA) tag was incorporated into the C-terminus of the original parent mouse periostin cDNA clone by PCR.

Immunocytochemistry and Western blotting

For immunocytochemistry, HH25 chick outflow tracts were dissected, pooled, and dispersed (trypsin-EDTA- Sigma). 1×10^4 cells were plated on collagen coated glass slides in M199 media supplemented with 1% insulin selenium transferrin (ITS), 100 U pen/strep, and 1% chick serum. Cells were grown in culture for 4 days, fixed in 4% paraformaldehyde and immunostained for periostin using a rabbit a-chick periostin antibody as described previously (Kern et al., 2005). Western blot analysis was further performed to verify that HH25 AV cushions are capable of being infected by the periostin adenoviruses and to ascertain levels of periostin expression within these tissues. HH25 AV cushions were dissected and placed in hanging drop cultures containing M199+ 100U pen/strep+1%ITS. The adenoviruses were then added to the droplets at an MOI of 50. After 4 days in culture, cushion explants were removed, spun ($1500 \times g$ for 5 min) and resuspended in 30 μl of $1 \times$ RIPA buffer containing a $1 \times$ protease inhibitor cocktail (Sigma). Samples were loaded onto a 4–15% gradient Tris–HCL protein gel (BIORAD), electrophoresed, blotted onto nitrocellulose and probed for periostin using a rabbit polyclonal α-mouse periostin antibody (1:2000) which reacts with chicken and mouse periostin as previously described in detail (Kruzynska-Frejtag et al., 2004). β-tubulin was used as a normalization control. Densitometric analysis was performed using NIH Image J software. A positive control Western was performed using media and cell lysates from infected and non-infected HEK293 cells. For these Western analyses, a mouse monoclonal HA antibody (HA-7 Sigma) was used at a 1:1000 dilution followed by a goat α-mouse secondary at a 1:10,000 dilution. Detection for all Western analyses used standard ECL detection (Upstate Biologicals).

Generation and purification of full-length periostin

Purified periostin was created by infecting 1×10^6 HEK293 cells with the mouse periostin over-expression (sense) virus (with HA tag) in serum-free conditions. Conditioned media were obtained after 3 days and adjusted to a final 0.5% Triton X-100, to which a cocktail of protease inhibitors was added. The medium was clarified by centrifugation (12,000 rpm; 10 min), then run over immobilized anti-HA beads (Vector Laboratories). The beads were extensively washed with 0.5% Triton X-100/PBS, then with PBS. Finally, bound periostin was eluted using 50 mM diethylamine. Peak levels of periostin eluted in the second bead volume of eluate. This periostin-rich fraction was neutralized by

addition of 1 M sodium phosphate pH 6.3 to a final concentration of 0.1 M. Quantification of purified protein was conducted by μ-BCA assay (Pierce).

Cushion mesenchyme adhesion and spreading

HH25 AV cushions were microdissected from the myocardial wall and trimmed of residual myocardium, digested with 0.05% Trypsin/EDTA (Invitrogen), pelleted by centrifugation, and reconstituted in serum free M199 (Invitrogen). Tissue culture wells were treated with collagen I, fibronectin, or purified periostin at concentrations ranging from 0.5–10 μg/ml for 4 h, followed by three rinses in PBS. Wells were then blocked with 1% BSA (Sigma) for 1 h, aspirated, and then 30,000 cells (in 100 μl) inoculated into each well. Cells were allowed to adhere for 1 h, followed by fixation in 10% ethanol/ 2% Crystal violet (Sigma) for 5 min. Non-adherent cells and free crystal violet were removed by 5 rinses with PBS (Sigma). Bound crystal violet was then released from adhered cells by 1:1 Ethanol/Phosphate buffer at pH 4.5. Absorbance was recorded by calorimeter at 525 nm, and adhered cell number was quantified from a calibration curve created using varying numbers of HH25 cushion cells adhered for 24 h. Degree of spreading was assessed by phase contrast image analysis of adherent cells using NIH Image software. Spread vs. non-spread cells were determined using a thresholding of the non-dimensional shape factor $S = 4\pi A / P^2$, with $S = 1$ denoting circular shape and 0 is a straight line ($A =$ cell area and $P =$ cell perimeter). Integrin dependency on cushion cell adhesion and spreading was assessed by repeating the above experiments in the presence of function blocking antibodies to $\alpha_v\beta_3$ or β_1 integrin pairs (Chemicon, 5 μg/ml).

Cushion mesenchyme migration and invasion

HH25 Cushion cells were isolated and dispersed as described above and divided into three aliquots of M199 containing 1% chick serum and ITS. Aliquots received adenovirus of sense periostin, antisense periostin, or LacZ control with an MOI=50. Cells were then aggregated by hanging drop (20,000 cells each) overnight. Drops were then placed on top of type I collagen gels (1.5 mg/ml) and allowed to adhere for 2 h before 400 μl of additional culture medium was added. Cushion cell migration and invasion proceeded for 72 h, after which the cells were fixed with 100% methanol overnight. Gels were then rinsed in 90%, 80%, 70%, and 50% methanol in PBS for 30 min each under gentle rocking, followed by 100% PBS overnight. Cell invasion was quantified manually at 80 μm depth into the gel and at 20 μm intervals deeper until no cells were observed. Integrin dependency on invasion was determined by identical experiments in the presence of blocking antibodies to either β_1 or $\alpha_v\beta_3$ integrins (5 μg/ml) as before. Effects of Rho kinase (p160ROCK) and PI 3-kinase on cell invasion were determined by identical experimentation in the presence of small molecule inhibitors Y-27632 (Calbiochem, 5 μM) or wortmannin (Calbiochem, 1 μM), respectively to the media. Immunostaining of gels was conducted with antibodies to β1 integrin (1:100, Chemicon), periostin (1:100, in house antibody; Kern et al., 2005), and α-smooth muscle actin (1:100, Spring Bioscience) and imaged using confocal microscopy. Lack of myocardial cell contamination was confirmed by MF20 staining (hybridoma serum 1:1).

Collagen matrix condensation

Type I collagen hydrogels (1.5 mg/ml density in M199 medium supplemented with 1% chick serum) were created by mixing soluble monomer solution with 2×10^5 HH25 cushion cells per milliliter (creating a homogeneous cell distribution), neutralizing the solution with 0.1 N NaOH, and immediately inoculating 250 microliters per cylindrical well (4-Well plates, Nunc). Neutralized collagen monomers formed solidified fibrous networks by 1 h of culture at 37°C, after which 400 μl of culture medium (M199 supplemented with 1% chick serum, 250 μg/ml insulin, 25 μg/ml transferrin, and 250 ng/ml selenious acid) was added. Additional gels were made supplemented with 2 μg/ml of purified periostin (kind gift of Dr. S. Lee, Biovendor) or purified fibronectin (kind gift of W. Argraves). Collagen gels were released from the walls of the wells after 12 h, and allowed to compact freely for 7 days, after which gels were fixed in 4% paraformaldehyde and stained for α-smooth muscle actin (αSMA, 1:100) and cardiac specific myosin MF20 (hybridoma

serum, 1:1). Images were generated using laser confocal microscopy at identical gain and offset settings. Additional experiments were conducted using cells infected with periostin over-expressing or anti-sense adenovirus (MOI=50), which were allowed to compact for 7 days, after which culture media changed with media that included signal pathway inhibitors Y-27632 (Rho kinase, 5 μM) or wortmannin (PI 3-kinase, 1 μM) for an additional 3 days of culture. In all experiments, matrix condensation was quantified by the ratio of compacted area to the day 0 original area.

Statistical analyses

At least four independent experiments were conducted per condition and the experiments were repeated at least twice using different batches of cell isolates and media. Analysis of variance (ANOVA) was used to determine significant differences between groups followed by pairwise comparisons using Tukey's modified t-test. $P < 0.05$ was considered significant for these analyses.

Results

Viral mediated expression and inhibition of periostin

Immunocytochemistry and Western blotting were performed to validate overexpression and knockdown of periostin using specific adenoviruses. Immunocytochemistry performed on cushion mesenchyme infected with the constitutively active full-length periostin expressing adenovirus showed a substantial increase in periostin expression when compared to the LacZ control. In addition, cells infected with the anti-sense periostin adenovirus showed negligible staining (Fig. 1A.). To quantify these findings, Western blot analysis was performed on AV cushion explants. Lysates infected with antisense periostin showed complete absence of the 90 and 37 kDa periostin protein variants (Fig. 1B, arrows). A third variant (∼75 kDa) did not show a significant decrease in expression. This may represent a more stable protein with a longer half-life thereby not being affected by the antisense virus. An increase in expression of the 90 kDa periostin variant was observed following infection with the periostin overexpressing adenovirus (arrowhead). Densitometric analysis demonstrated that there was a 2.2-fold increase over endogenous levels of periostin. To further verify that the 90 kDa band was generated by the overepxressing virus, HEK293 cells were infected with periostin and immunoblotted for HA (tag at the carboxyl terminus of the adenovirally produced protein) (Fig. 1C). Only the infected cells and media show an immunopositive band for periostin. This demonstrates/validates three important points: (i) the virus is competent to produce periostin, (ii) periostin is secreted (media fraction), and (iii) periostin is present in the cellular fraction suggesting its ability to be a matricellular protein.

The periostin expressing adenovirus (PNOX) produced and secreted a 90 kDa full-length periostin as detected by immunoblotting with an anti-HA antibody (Fig. 1C). Based on densitometric analysis of blots using standard curves, it was determined that affinity purification of periostin infected lysates resulted in nearly 100% homogenous soluble periostin migrating at the theoretical full-length MW (90 kDa) at a concentration of about 35 μg/ml (Fig. 1D).
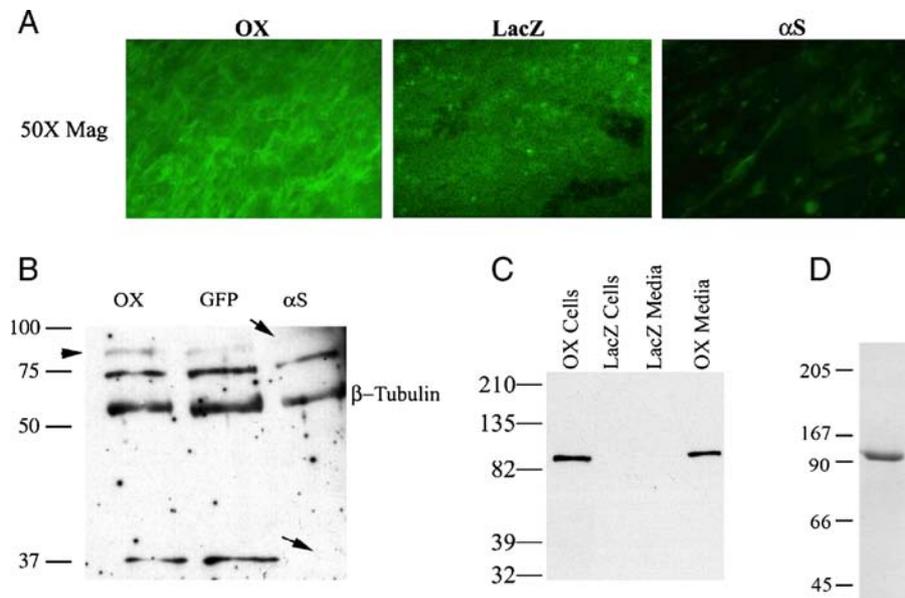
Fig. 1. Validation of periostin virus expression and protein purification. (A) Immunohistochemical validation of periostin overexpression and knockdown in HH26 outflow tract cells by sense and antisense adenovirus as compared to LacZ control. A significant increase in periostin positive cells is evident in the PNOX cells whereas little appreciable staining is seen in the αS. (B) Western blot of infected HEK293 cells with the periostin overexpressing adenovirus. Expression of the 90 kDa adenovirally produced periostin protein is clearly demonstrated in the HEK293 supernatant. Non-infected control shows antibody specificity. (C) Functional validation of the periostin adenoviruses in HH25 AV cushion tissue. An overexpression (2.2 net increase) of the 90 kDa adenovirally expressed variant of periostin (OX) is seen when compared to the endogenous levels (GFP). Infection with the αS periostin adenovirus resulted in a complete absence of the 90 kDa and the 37 kDa variants. No change was observed in a 75 kDa periostin variant. β-tubulin was used as a normalization control. For both blots (B and C), the α-mouse periostin antibody was utilized. (D) Purification of full-length periostin from HEK293 cells determined by Western blot. Two micrograms of periostin purified as described in the Materials and methods was resolved by SDS-PAGE and detected by Coomassie blue staining. Only one band was present at the 90 kDa, demonstrating the purity of the periostin preparation.

Integrin mediated adhesion and spreading to periostin

HH25 AV Cushion mesenchyme adhered to collagen I, fibronectin, and periostin in a dose-dependent manner. Maximal adhesion for all proteins studied was reached at 2 μg/ml concentrations (Fig. 2). Adhesion of cushion cells to periostin was generally less to that of collagen I or fibronectin, particularly at the 0.5 μg/ml concentration. Cushion cells spread significantly less on periostin than collagen I or fibronectin at 0.5 μg/ml. Fewer than 14% of cushion cells were spread on 0.5 μg/ml periostin, but spreading increased to 81% of cells at 10 μg/ml. Cushion cell spreading was not dependent on collagen concentration since approximately half of the cells spread at both concentrations tested. *Adhesion* to periostin but not fibronectin was significantly reduced with antibodies to either $\alpha_v\beta_3$ or β_1 integrin pairs, but no modulation of adhesion to fibronectin was observed at these dilutions (Fig. 3). *Spreading* in response to periostin, however, was only reduced by antibodies to $\alpha_v\beta_3$ integrins, and no modulation to spreading on fibronectin was observed with either of the integrin antibodies. These results demonstrate that AV cushion cells are sensitive to periostin concentration in terms of modulating their adhesion and spreading response through specific integrin binding.

Cushion mesenchyme invasion enhanced by periostin

HH25 AV cushion mesenchyme invaded collagen gels over 72 h such that the numbers of cells present in a tissue plane decreased monotonically with depth (Supplemental Fig. 2). Lack of MF20 expression confirmed no contaminating cardiomyocytes (Supplemental Fig. 3). Overexpression of periostin (PN OX) significantly enhanced the number of invaded cells (measured at −80 μm depth) over LacZ infected controls (Fig. 4). Infection of antisense periostin (PN αS) reduced the number of invading mesenchyme significantly below that of LacZ controls. No significant differences were seen in surface migration area between conditions (Supplemental Fig. 4). Cells that remained on the surface (regardless of treatment) were polygonal in shape with circumferential actin fiber expression, except at the periphery where the migrating cell front contained radially oriented cells with prominent actin stress fiber formation (Fig. 5). Periostin expression was colocalized with migratory and invasive cell morphology concomitant with increased α-smooth muscle actin and β1 integrin expression. Both β_1 and $\alpha_v\beta_3$ integrin signaling mediated cushion mesenchyme invasion by periostin (Fig. 6). Blocking β_1 integrin signaling resulted in over 50% reduction in the number of invaded cells seen in LacZ controls, and blocking $\alpha_v\beta_3$ signaling resulted in almost 80% reduction. Mesenchyme invasion was enhanced with constitutively active periostin adenovirus (PNOX) as before, with reductions of 40% and 50% with anti-β_1 and anti-$\alpha_v\beta_3$ antibodies, respectively. Unlike the LacZ controls, disruption of $\alpha_v\beta_3$ signaling in PNOX cultures did not result in significantly less invaded cells over β_1. Signal pathway dependence on cushion cell migration and invasion was modified by supplementing media of viral treated aggregates with inhibitors to Rho
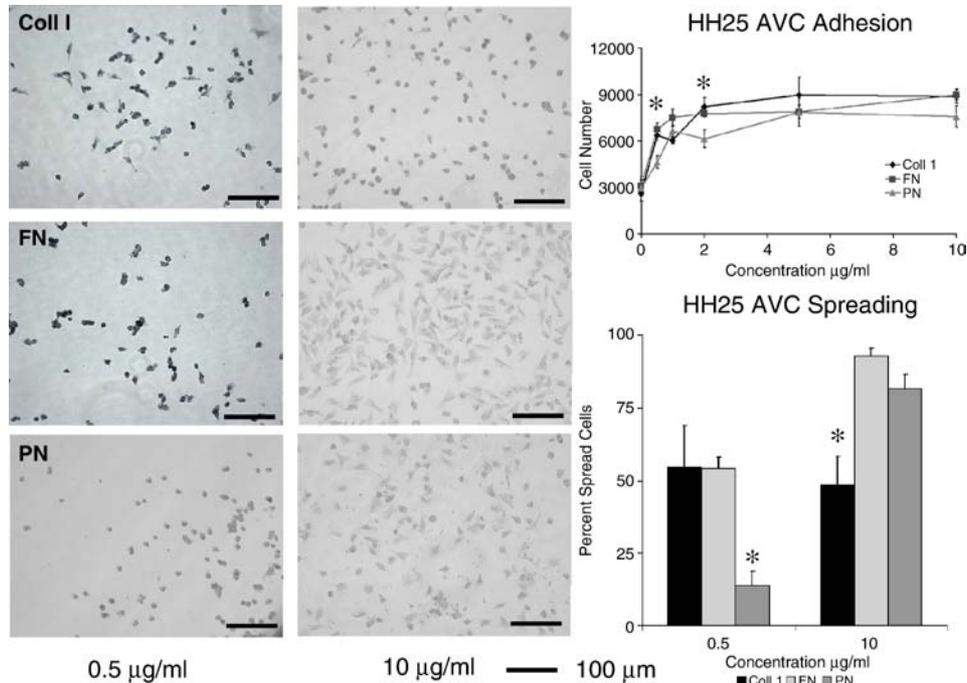
Fig. 2. Adhesion and spreading of HH25 atrioventricular cushion mesenchyme to different doses of extracellular matrix proteins type I collagen (Coll I), fibronectin (FN), and periostin (PN). * Denotes significance at $P<0.05$.

kinase (Y-27632) or PI 3-kinase (Wortmannin). Specifically, addition of Y-27632 to PNOX infected cultures reduced cell invasion to control levels, suggesting that this invasion was mediated by RhoA signaling (Fig. 7). Wortmannin reduced mesenchymal cell invasion regardless of periostin treatment condition, suggesting that PI 3-kinase is also involved in this process. Invaded cells in the presence of wortmannin were almost uniformly rounded while cells in Y-27632 maintained migratory morphology (Supplemental Fig. 5), suggesting that PI 3-kinase is also involved in filipodia extension and actin rearrangement for migration in these cells. No immunohisto-chemically detectable difference in $\beta1$ integrin expression was observed with Rho kinase inhibition, suggesting that integrin signaling is upstream of Rho kinase activity.

Periostin enhances matrix condensation

HH25 cushion mesenchyme homogeneously distributed inside collagen gels compacted the matrix over a 7 day period (Fig. 8). Supplementation of the collagen matrix with 2 µg/ml periostin (homogeneously mixed in with the cells and collagen prior to gelation) resulted in significantly increased condensa-tion at 6 days over collagen alone and collagen supplemented with 2 µg/ml fibronectin (52% vs. 37% vs. 28% of original area respectively, $P<0.05$). Immunohistochemistry of these constructs suggests enhanced α-smooth muscle actin expres-sion in the supplemented (fibronectin or periostin) matrix compared with collagen controls, implying that matrix con-densation may be related to the expression of contractile
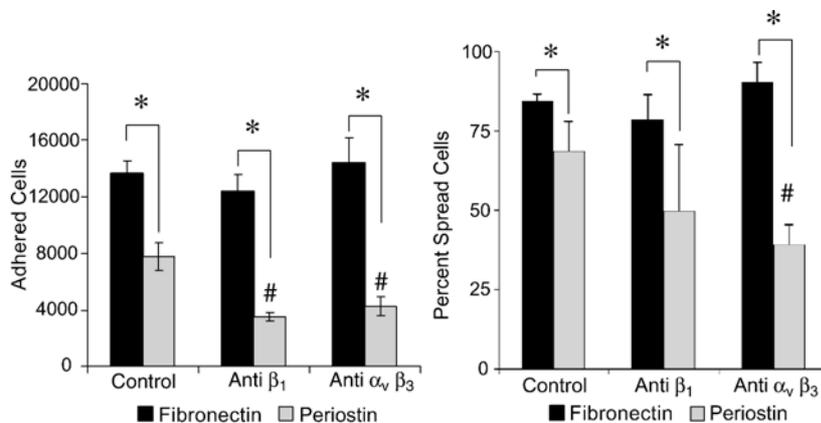

Fig. 3. Adhesion to periostin (but not fibronectin) is dependent on $\alpha_v\beta_3$ and β_1 integrins. 30,000 cushion mesenchyme cells were allowed to adhere for 1 h in the presence of blocking antibodies used at 5 µg/ml concentration. * Denotes significant difference between matrix proteins ($P<0.05$), while # denotes significant between treatments ($P<0.05$).
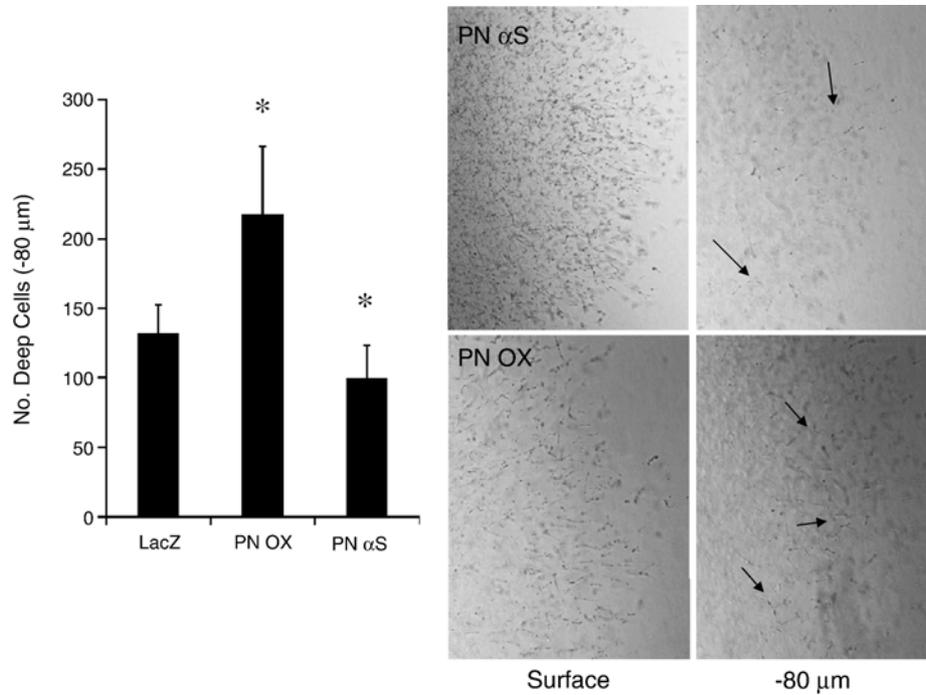
Fig. 4. Periostin overexpression enhances cushion mesenchyme invasion (arrows) over LacZ controls while antisense reduces invasion. * Denotes significance $P < 0.05$.

proteins in mesenchyme. Lack of MF20 expression in any constructs confirmed that there was no contamination by cardiomyocytes (Supplemental Fig. 3). Additional experiments were conducted enhancing endogenous constitutive expression of periostin through adenovirus delivery and the same results were achieved ($\sim$20% of original area in PNOX gels vs. $\sim$50% in PNαS gels). To test the dependency of compaction on signal pathways, gels were treated with a combination of constitutively active periostin adenovirus (expressing vs. anti-sense) for 7 days followed by the addition of inhibitors Y-27632 (Rho kinase) or wortmannin (PI 3-kinase) for an additional three days. Both Rho kinase and PI 3-kinase inhibition resulted in reduced compaction compared to controls in PNαS gels, suggesting that compaction of collagen alone is dependent on both pathways in cushion mesenchyme (Fig. 9). However, PI 3-kinase inhibition resulted in a complete block in condensation compared to controls and
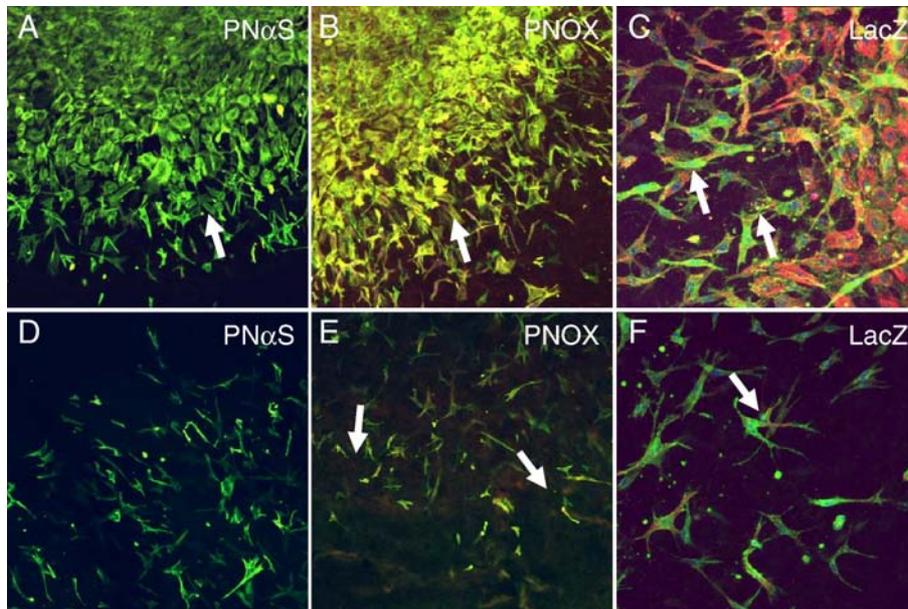

Fig. 5. Immunohistochemistry of surface (0 μm, A–C) and deep (−80 μm, D–F) sections of invading HH25 AV cushion mesenchyme. PNαS infected cultures exhibited almost no detection of periostin (red) in either surface (A) or deep cells (D). PNOX infected cultures coexpressed periostin (red) and a-smooth muscle actin (green) in migratory/invasive morphology in both surface (B) and deep cells (E). β1 integrin (green) expression was also colocalized with a-smooth muscle actin (red) in migratory/invasive cells at both surface (C) and deep levels (F). All images are at 200× magnification.
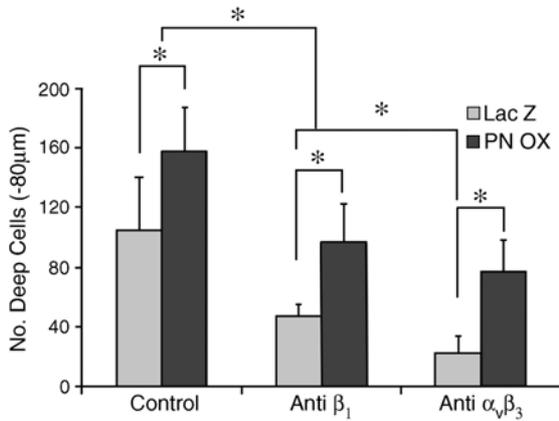
Fig. 6. Cushion mesenchyme invasion into collagen I gels is dependent on integrins. Blocking antibodies to $\alpha_v\beta_3$ or β_1 integrins (5 μg/ml) were added to culture medium and resulted in reduced invasion from both LacZ control and periostin overexpressing cultures. * Denotes significance at $P < 0.05$.

Rho kinase inhibition (between which there were no significant differences), suggesting that PI 3-kinase is necessary for periostin mediated condensation.

Discussion

The results of this study identify new mechanisms by which atrioventricular cushion mesenchyme remodels itself into valvular tissue, and highlights the previously unknown role periostin plays in this process. Valvulogenesis is thought to be regulated by a complex coordination of growth factor signaling and extracellular matrix interactions (Camenisch et al., 2002; Schroeder et al., 2003), much of which is currently not known. Early stage mesenchymal transformation requires the downregulation of myocardial VEGF and upregulation of BMP, which in turn stimulates the endocardial expression of TGFβ resulting in endocardial hypertrophy, activation, and invasion into the cardiac jelly (Chang et al., 2004; Dor et al., 2003; Sugi et al., 2004; Yamagishi et al., 1999). In order for prevalvular cushions to elongate into thin fibrous leaflets, endo-cardial VEGF signaling must be activated and BMP signaling repressed (Chang et al., 2004; Jackson et al., 2003; Sanford et al., 1997). A mechanism for this has not been identified, but may possibly be through cellular interactions with extracellular matrix, including periostin. Lincoln et al. assessed the response of HH25 atrioventricular mesenchyme to growth factor stimulation, and found that BMP-2 upregulated sox9 expression through smad 1/5/8 phosphorylation while FGF-2 induced tenascin and scleraxis expression (Lincoln et al., 2006a). These pathways are similar to the development of cartilage (BMP) and tendon (FGF), suggesting that valve leaflet development may rely on similar pathways (yet they normally do not form cartilage) (Lincoln et al., 2006b).

We (and others) have previously implicated periostin as an important regulator of fibroblastic differentiation in regions that have the capacity to form bone, such as the periodontal ligament and periosteum (Horiuchi et al., 1999; Kruzynska-Frejtag et al., 2001, 2004). Periostin is specifically expressed in cushion mesenchyme throughout the remodeling period, with particu-

larly enhanced expression in the cushion subendocardium and cushion–myocardial interfaces (Kern et al., 2005; Lindsley et al., 2005; Norris et al., 2004). Periostin is also upregulated by growth factor signaling, including TGFβ, BMP, and PDGF (Horiuchi et al., 1999; Li et al., 2005; Lindner et al., 2005). Periostin null mice exhibit early onset periodontal disease due to improper mesenchymal to fibroblastic transformation in these regions, as well as reduced heart ventricular volumes and reductions in trabecular bone densities (Kii et al., 2006; Rios et al., 2005). Approximately 20% of these mice die within 2 weeks of birth from valvular insufficiency. Placing mice on a soft diet alleviated part of the periodontal degeneration with periostin deficiency, suggesting that mechanics plays a role in periostin mediated responses. We therefore postulated that periostin may be an important regulator of post-EMT cushion remodeling. The studies presented here demonstrated that periostin plays a functional role in mediating mesenchymal cell migration/invasion and matrix condensation. These actions were mediated by $\alpha_v\beta_3$ and β_1 integrin adhesion based signaling through Rho/PI 3-kinase pathways. Cell migration, invasion, and condensation through periostin were associated with enhanced α-smooth muscle actin expression. It is important to note that the effects of periostin overexpression were much more exuberant than its knock down. This is likely due to the fact that cushion mesenchymal cells migrate through collagen without the presence of periostin during early cushion formation (Kern et al., 2005; Norris et al., 2004). Continued maturation of the cushions into fibrous leaflets would then require the expression of additional proteins including periostin to enhance migration and matrix condensation. Therefore, a basal level of these functions occurs without periostin, but not enough to ensure proper valve development as evidenced by the aforementioned periostin knockout studies in mice.

Three-dimensional culture models are important tools for studying cell–matrix interactions because of the differences in conformation apparent in protein networks but not mimicked by two dimensional culture (Grinnell, 2003; Shreiber et al., 2001).
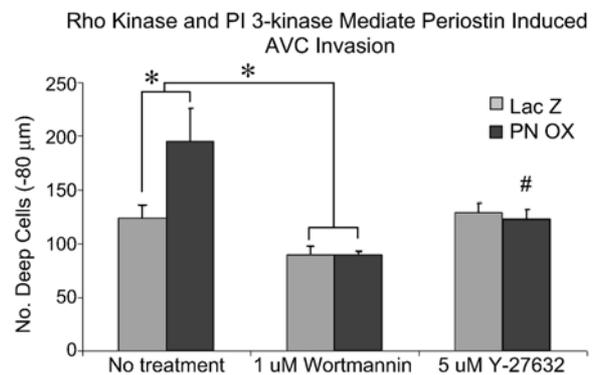

Fig. 7. Cushion mesenchyme invasion into collagen I gels is dependent on Rho/PI 3-kinase. PI 3-kinase inhibitor (Wortmannin) resulted in reduced numbers of invaded cells over controls, with a greater reduction of invasion in PNOX cultures. Rho kinase was not involved in control cell invasion, but inhibition of Rho kinase with Y-27632 in PNOX cultures results in a reduction of invaded cells back to control levels. * Denotes significance at $P < 0.05$, # denotes significantly different from no treatment control.
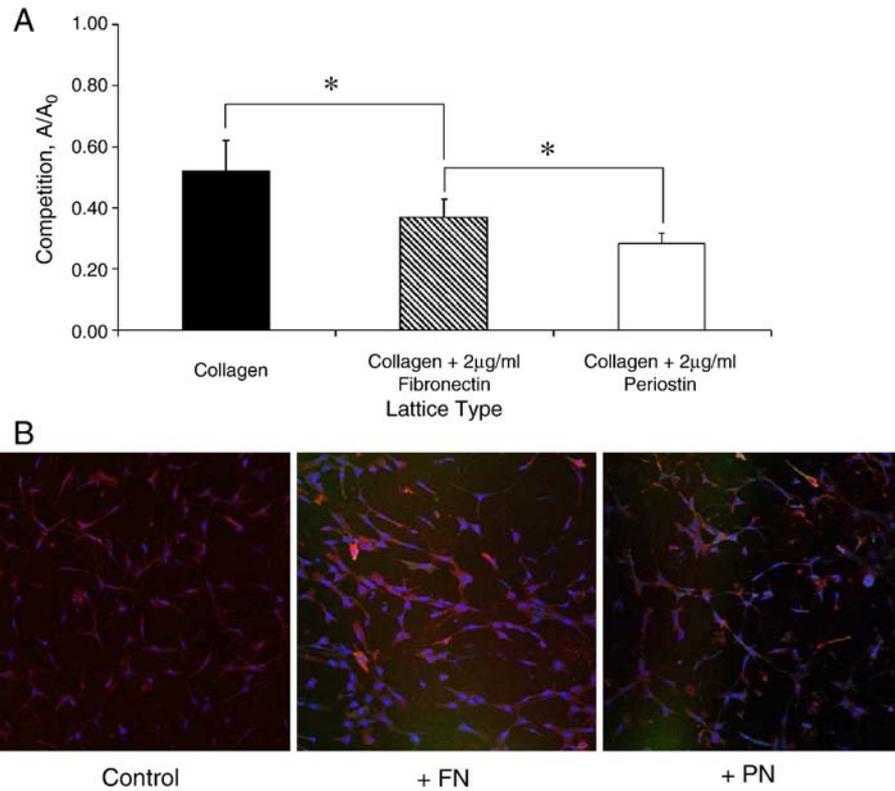
Fig. 8. Condensation of collagen I matrix by HH25 AV cushion mesenchyme. (A) Supplementation with purified fibronectin (FN, 2 μg/ml) or periostin (PN, 2 μg/ml) resulted in enhanced condensation, with periostin supplemented constructs compacting the most. (B) Enhanced matrix condensation is associated with increased expression of α-smooth muscle actin. FN and PN supplemented collagen I gels had significantly greater expression compared to collagen I only controls. * Denotes significance at $P < 0.05$.

Grinnell and coworkers have developed and compared models of tissue development and found that free floating gels best represent fibrous tissue development while mechanically constrained gels develop myofibroblast phenotypes associated with wound healing and scar formation (Grinnell and Ho, 2002). TGFβ was shown to enhance the compaction of floating gels, but not stressed gels, with an associated increase in α-smooth muscle actin expression. This model system has been employed
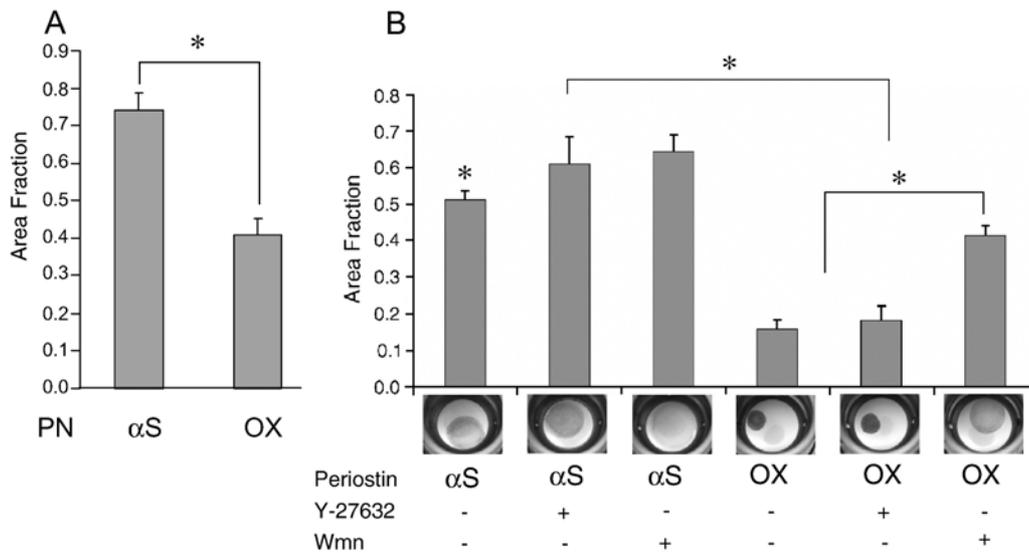

Fig. 9. Effects of Rho/PI 3-kinase inhibition on matrix condensation by periostin overexpressing cushion mesenchyme. (A) Increased matrix compaction after 7 days by periostin overexpressing constructs compared to antisense periostin. (B) Matrix compaction after an additional three days incubation with Rho kinase inhibitor Y-27632 (5 μM) or PI 3-kinase inhibitor Wortmannin (Wmn, 1 μM). "+" denotes addition of the inhibitor, "−" without inhibitor. αS = antisense, OX = overexpression. * Denotes significance $P < 0.05$.

using various cell types and exogenous addition of extracellular matrix proteins such as fibronectin and vitronectin, which both appear to have a permissive effect on matrix compaction by cells mediated by specific integrin pairs (Borck et al., 2004; Nakamura et al., 2003; Scaffidi et al., 2001; Taliana et al., 2000). We propose that this model can also be applied to valvular development, by which undifferentiated mesenchyme in a highly porous, low density collagenous matrix condenses and matures into fibroblasts populating thin fibrous leaflets.

Periostin expression has been associated with several pathological conditions known for mesenchymal cell proliferation and migratory invasion, namely fibrotic diseases and cancer. Periostin virus infected hearts developed dilative cardiomyopathy with decreased numbers of myocytes and increased collagen deposition (Katsuragi et al., 2004). Vascular injury also upregulated periostin expression in the neointima concomitant with smooth muscle cell migration, potentially by altered FGF-2 and TGFβ release (Li et al., 2005). Periostin has recently been shown to influence mesenchymal transformation, migration, and invasion in several cancer cell lines. Adhesion to periostin was mediated by $\alpha_v\beta_3$ or $\alpha_v\beta_5$ integrins, but metastatic tumor growth was mediated through $\alpha_v\beta_3$ (Gillan et al., 2002). This growth was caused by periostin induced upregulation of the VEGF receptor Flk1 (Shao et al., 2004). Analysis of βig-H3, another fasciclin family member with high homology to periostin, identified several integrin binding motifs in these domains, including $\alpha_3\beta_1$, $\alpha_v\beta_3$ and $\alpha_v\beta_5$, both of which confer functionality (Kim et al., 2002; Nam et al., 2003; Park et al., 2004). Some of these were also identified in periostin, though a complete analysis of this protein has not been done. Where periostin induced fibroblast transformation and matrix invasion, it was also shown to upregulate MMP-9 and EGFR expression (Yan and Shao, 2006). In our studies, we show that periostin mediates cushion cell matrix remodeling through invasion and condensation mediated by Rho/PI 3-kinase signaling and integrin binding. Periostin expression therefore must be tightly controlled to ensure proper valvular development. Limited periostin expression likely results in a persistence of undifferentiated mesenchyme in cushions, while an overabundance may lead to overproduction of fibrous tissue and a possible progression towards osteogenic differentiation (Litvin et al., 2004). Interestingly, adult valve interstitial cells express periostin, whereas valvular endothelial cells do not, suggesting that this complex form of periostin regulation extends into adulthood (Butcher et al., 2004).

Cushion mesenchyme invades collagen matrix mediated by integrin signaling through the Rho/PI 3-kinase pathway (Fig. 10). Periostin enhances this function, but this appears to be Rho kinase-dependent. Cushion cells compact collagen matrix mediated by Rho/PI 3-kinase, associated with enhanced α-smooth muscle actin expression. Periostin enhances this compaction, but this was PI 3-kinase-dependent. Rho kinase and PI 3-kinase pathways are important for a variety of matrix interactions in many cell types, but these pathways can be heterogeneously regulated. Corneal endothelial cells require both inactivated Rho and PI 3-kinase activity to migrate, while fibroblast invasion required Rho but not PI 3-kinase (Lee et al., 2006). Vascular smooth muscle cell mediated gel compaction is reduced by either Rho kinase or PI 3-kinase inhibition, but is more sensitive to Rho (Li et al., 2003). IGF-1 promoted cancer
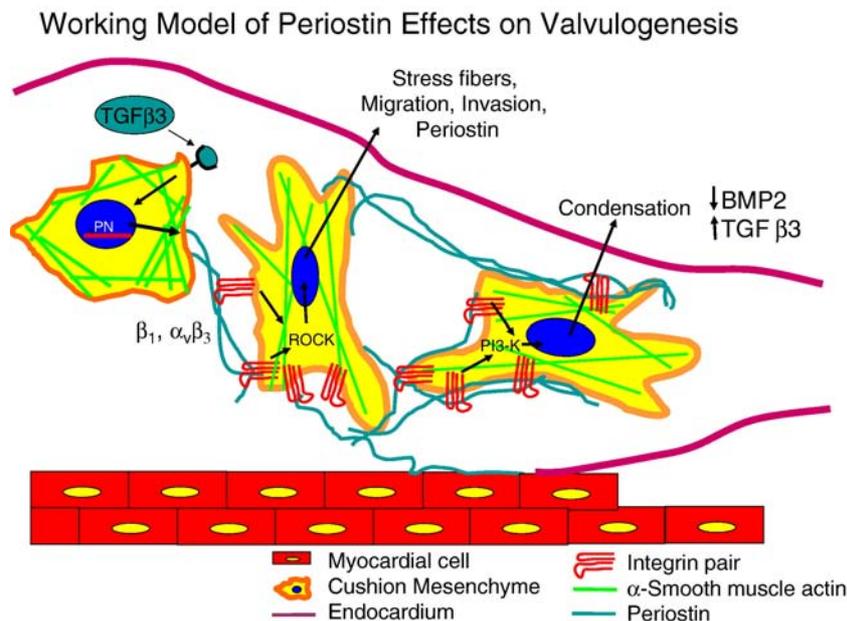

Fig. 10. Schematic detailing the proposed roles of periostin in mediating post-EMT cushion remodeling. After EMT (approximately HH20 in chick) a signaling ligand (our preliminary evidence suggests it is TGFβ3) signals mesenchymal cells to synthesize and secrete periostin. Mesenchyme then adhere to periostin via β_1 and $\alpha_v\beta_3$ integrin pairs and further invade and migrate within the collagenous cushion matrix via Rho kinase signaling, stress fiber formation, and filipodia extension. By HH25, cushion tissue is fully mesenchymalized and the resident cells begin to condense the matrix, this process enhanced by periostin signaling via PI-3 kinase. This condensation contributes to thinning the cushions into fibrous leaflets and delaminating the tissue from the myocardial wall by an as yet unknown mechanism, but possibly related to the upregulation of TGFβ3 and downregulation of BMP2 in chick.

cell transmigration through the Rho/PI 3-kinase pathway, but independent of Akt signaling (Qiang et al., 2004). Periostin-induced smooth muscle cell neointimal migration from vascular injury was dependent on PI 3-kinase signaling (Li et al., 2005). Based on these studies and our results, we believe periostin induced invasion and matrix condensation may be differentially regulated by Rho and PI 3-kinase, with Rho mediating invasion and PI 3-kinase regulating condensation. Differential regulation of cell function through this pathway has been demonstrated before in other cell types (Banyard et al., 2000). This is likely through differences in integrin based adhesion signaling and growth factor response, though the effects of mechanical forces cannot be ruled out.

Taken together, these results highlight the similar role periostin plays in morphogenesis of mesenchymal tissues in normal and pathological conditions. Schroeder et al. identified the extracellular matrix as a key understudied component for conferring signal pathway switching in valvulogenesis by (1) binding and releasing growth factors and/or (2) adhesion based signaling through focal adhesions (Schroeder et al., 2003). These non-structural constituents have been termed "matricellular" proteins (Bornstein and Sage, 2002). Based on these studies, we believe that the function of periostin is consistent with this definition and is an important mediator of cushion remodeling.

Acknowledgments

Appendix A. Supplementary data

Supplementary data associated with this article can be found, in the online version, at doi:10.1016/j.ydbio.2006.09.048.

References

Baldwin, H.S., Lloyd, T.R., Solursh, M., 1994. Hyaluronate degradation affects ventricular function of the early postlooped embryonic rat heart in situ. Circ. Res. 74, 244–252.

Banyard, J., Anand-Apte, B., Symons, M., Zetter, B.R., 2000. Motility and invasion are differentially modulated by Rho family GTPases. Oncogene 19, 580–591.

Borck, A., Massey, E., Loftis, M.J., Carver, W., 2004. Exposure of cardiac fibroblasts to the herbicide nitrofen causes altered interactions with the extracellular matrix. Cell Biol. Toxicol. 20, 15–24.

Bornstein, P., Sage, E.H., 2002. Matricellular proteins: extracellular modulators of cell function. Curr. Opin. Cell Biol. 14, 608–616.

Butcher, J.T., Penrod, A.M., Garcia, A.J., Nerem, R.M., 2004. Unique morphology and focal adhesion development of valvular endothelial cells in static and fluid flow environments. Arterioscler., Thromb., Vasc. Biol. 24, 1429–1434.

Camenisch, T.D., Spicer, A.P., Brehm-Gibson, T., Biesterfeldt, J., Augustine, M.L., Calabro Jr., A., Kubalak, S., Klewer, S.E., McDonald, J.A., 2000. Disruption of hyaluronan synthase-2 abrogates normal cardiac morphogenesis and hyaluronan-mediated transformation of epithelium to mesenchyme. J. Clin. Invest. 106, 349–360.

Camenisch, T.D., Schroeder, J.A., Bradley, J., Klewer, S.E., McDonald, J.A., 2002. Heart-valve mesenchyme formation is dependent on hyaluronan-augmented activation of ErbB2–ErbB3 receptors. Nat. Med. 8, 850–855.

Chang, C.P., Neilson, J.R., Bayle, J.H., Gestwicki, J.E., Kuo, A., Stankunas, K., Graef, I.A., Crabtree, G.R., 2004. A field of myocardial–endocardial NFAT signaling underlies heart valve morphogenesis. Cell 118, 649–663.

De la Cruz, M.V., Markwald, R.R., 2000. Embryological development of the ventricular inlets. Septation and atrioventricular valve apparatus. In: De la Cruz, M.V., Markwald, R.R. (Eds.), Living Morphogenesis of the Heart. Birkhauser, Boston, pp. 131–157.

de Lange, F.J., Moorman, A.F., Anderson, R.H., Manner, J., Soufan, A.T., de Gier-de Vries, C., Schneider, M.D., Webb, S., van den Hoff, M.J., Christoffels, V.M., 2004. Lineage and morphogenetic analysis of the cardiac valves. Circ. Res. 95, 645–654.

Dor, Y., Klewer, S.E., McDonald, J.A., Keshet, E., Camenisch, T.D., 2003. VEGF modulates early heart valve formation. Anat. Rec. A Discov. Mol. Cell Evol. Biol. 271, 202–208.

Funderburg, F.M., Markwald, R.R., 1986. Conditioning of native substrates by chondroitin sulfate proteoglycans during cardiac mesenchymal cell migration. J. Cell Biol. 103, 2475–2487.

Garcia-Martinez, V., Sanchez-Quintana, D., Hurle, J.M., 1991. Histochemical and ultrastructural changes in the extracellular matrix of the developing chick semilunar heart valves. Acta Anat. (Basel) 142, 87–96.

Gillan, L., Matei, D., Fishman, D.A., Gerbin, C.S., Karlan, B.Y., Chang, D.D., 2002. Periostin secreted by epithelial ovarian carcinoma is a ligand for alpha (V)beta(3) and alpha(V)beta(5) integrins and promotes cell motility. Cancer Res. 62, 5358–5364.

Grinnell, F., 2003. Fibroblast biology in three-dimensional collagen matrices. Trends Cell Biol. 13, 264–269.

Grinnell, F., Ho, C.H., 2002. Transforming growth factor beta stimulates fibroblast–collagen matrix contraction by different mechanisms in mechanically loaded and unloaded matrices. Exp. Cell Res. 273, 248–255.

Hamburger, V., Hamilton, H.L., 1992. A series of normal stages in the development of the chick embryo. Dev. Dyn. 231–272 (1951).

Horiuchi, K., Amizuka, N., Takeshita, S., Takamatsu, H., Katsuura, M., Ozawa, H., Toyama, Y., Bonewald, L.F., Kudo, A., 1999. Identification and characterization of a novel protein, periostin, with restricted expression to periosteum and periodontal ligament and increased expression by transforming growth factor beta. J. Bone Miner. Res. 14, 1239–1249.

Hurle, J.M., Kitten, G.T., Sakai, L.Y., Volpin, D., Solursh, M., 1994. Elastic extracellular matrix of the embryonic chick heart: an immunohistological study using laser confocal microscopy. Dev. Dyn. 200, 321–332.

Jackson, L.F., Qiu, T.H., Sunnarborg, S.W., Chang, A., Zhang, C., Patterson, C., Lee, D.C., 2003. Defective valvulogenesis in HB-EGF and TACE-null mice is associated with aberrant BMP signaling. EMBO J. 22, 2704–2716.

Katsuragi, N., Morishita, R., Nakamura, N., Ochiai, T., Taniyama, Y., Hasegawa, Y., Kawashima, K., Kaneda, Y., Ogihara, T., Sugimura, K., 2004. Periostin as a novel factor responsible for ventricular dilation. Circulation 110, 1806–1813.

Kern, C.B., Hoffman, S., Moreno, R., Damon, B.J., Norris, R.A., Krug, E.L., Markwald, R.R., Mjaatvedt, C.H., 2005. Immunolocalization of chick periostin protein in the developing heart. Anat. Rec. A Discov. Mol. Cell Evol. Biol. 284, 415–423.

Kii, I., Amizuka, N., Minqi, L., Kitajima, S., Saga, Y., Kudo, A., 2006. Periostin is an extracellular matrix protein required for eruption of incisors in mice. Biochem. Biophys. Res. Commun. 342, 766–772.

Kim, J.E., Jeong, H.W., Nam, J.O., Lee, B.H., Choi, J.Y., Park, R.W., Park, J.Y., Kim, I.S., 2002. Identification of motifs in the fasciclin domains of the transforming growth factor-beta-induced matrix protein betaig-h3 that interact with the alphavbeta5 integrin. J. Biol. Chem. 277, 46159–46165.

Krug, E.L., Runyan, R.B., Markwald, R.R., 1985. Protein extracts from early embryonic hearts initiate cardiac endothelial cytodifferentiation. Dev. Biol. 112, 414–426.

Kruzynska-Frejtag, A., Machnicki, M., Rogers, R., Markwald, R.R., Conway,

S.J., 2001. Periostin (an osteoblast-specific factor) is expressed within the embryonic mouse heart during valve formation. Mech. Dev. 103, 183–188.

Kruzynska-Frejtag, A., Wang, J., Maeda, M., Rogers, R., Krug, E., Hoffman, S., Markwald, R.R., Conway, S.J., 2004. Periostin is expressed within the developing teeth at the sites of epithelial–mesenchymal interaction. Dev. Dyn. 229, 857–868.

Lee, Y.M., Cope, J.J., Ackermann, G.E., Goishi, K., Armstrong, E.J., Paw, B.H., Bischoff, J., 2006. Vascular endothelial growth factor receptor signaling is required for cardiac valve formation in zebrafish. Dev. Dyn. 235, 29–37.

Li, S., Moon, J.J., Miao, H., Jin, G., Chen, B.P., Yuan, S., Hu, Y., Usami, S., Chien, S., 2003. Signal transduction in matrix contraction and the migration of vascular smooth muscle cells in three-dimensional matrix. J. Vasc. Res. 40, 378–388.

Li, G., Oparil, S., Sanders, J.M., Zhang, L., Dai, M., Chen, L.B., Conway, S.J., McNamara, C.A., Sarembock, I.J., 2005. Phosphatidylinositol-3-kinase signaling mediates vascular smooth muscle cell expression of periostin in vivo and in vitro. Atherosclerosis.

Lincoln, J., Alfieri, C.M., Yutzey, K.E., 2004. Development of heart valve leaflets and supporting apparatus in chicken and mouse embryos. Dev. Dyn. 230, 239–250.

Lincoln, J., Alfieri, C.M., Yutzey, K.E., 2006a. BMP and FGF regulatory pathways control cell lineage diversification of heart valve precursor cells. Dev. Biol. 292, 292–302.

Lincoln, J., Lange, A.W., Yutzey, K.E., 2006b. Hearts and bones: shared regulatory mechanisms in heart valve, cartilage, tendon, and bone development. Dev. Biol.

Lindner, V., Wang, Q., Conley, B.A., Friesel, R.E., Vary, C.P., 2005. Vascular injury induces expression of periostin: implications for vascular cell differentiation and migration. Arterioscler., Thromb., Vasc. Biol. 25, 77–83.

Lindsley, A., Li, W., Wang, J., Maeda, N., Rogers, R., Conway, S.J., 2005. Comparison of the four mouse fasciclin-containing genes expression patterns during valvuloseptal morphogenesis. Gene Expression Patterns 5, 593–600.

Litvin, J., Selim, A.H., Montgomery, M.O., Lehmann, K., Rico, M.C., Devlin, H., Bednarik, D.P., Safadi, F.F., 2004. Expression and function of periostin-isoforms in bone. J. Cell. Biochem. 92, 1044–1061.

Litvin, J., Zhu, S., Norris, R., Markwald, R., 2005. Periostin family of proteins: therapeutic targets for heart disease. Anat. Rec. A Discov. Mol. Cell Evol. Biol. 287, 1205–1212.

Manasek, F.J., Reid, M., Vinson, W., Seyer, J., Johnson, R., 1973. Glycosaminoglycan synthesis by the early embryonic chick heart. Dev. Biol. 35, 332–348.

Mjaatvedt, C.H., Yamamura, H., Capehart, A.A., Turner, D., Markwald, R.R., 1998. The Cspg2 gene, disrupted in the hdf mutant, is required for right cardiac chamber and endocardial cushion formation. Dev. Biol. 202, 56–66.

Nakamura, Y., Sagara, T., Seki, K., Hirano, S., Nishida, T., 2003. Permissive effect of fibronectin on collagen gel contraction mediated by bovine trabecular meshwork cells. Invest. Ophthalmol. Visual Sci. 44, 4331–4336.

Nam, J.O., Kim, J.E., Jeong, H.W., Lee, S.J., Lee, B.H., Choi, J.Y., Park, R.W., Park, J.Y., Kim, I.S., 2003. Identification of the alphavbeta3 integrin-interacting motif of betaig-h3 and its anti-angiogenic effect. J. Biol. Chem. 278, 25902–25909.

Norris, R.A., Kern, C.B., Wessels, A., Moralez, E.I., Markwald, R.R., Mjaatvedt, C.H., 2004. Identification and detection of the periostin gene in cardiac development. Anat. Rec. A Discov. Mol. Cell Evol. Biol. 281, 1227–1233.

Oosthoek, P.W., Wenink, A.C., Vrolijk, B.C., Wisse, L.J., DeRuiter, M.C., Poelmann, R.E., Gittenberger-de Groot, A.C., 1998a. Development of the atrioventricular valve tension apparatus in the human heart. Anat. Embryol. (Berl.) 198, 317–329.

Oosthoek, P.W., Wenink, A.C., Wisse, L.J., Gittenberger-de Groot, A.C., 1998b. Development of the papillary muscles of the mitral valve: morphogenetic background of parachute-like asymmetric mitral valves and other mitral valve anomalies. J. Thorac. Cardiovasc. Surg. 116, 36–46.

Park, S.J., Park, S., Ahn, H.C., Kim, I.S., Lee, B.J., 2004. Conformational resemblance between the structures of integrin-activating pentapeptides derived from betaig-h3 and RGD peptide analogues in a membrane environment. Peptides 25, 199–205.

Person, A.D., Klewer, S.E., Runyan, R.B., 2005. Cell biology of cardiac cushion development. Int. Rev. Cytol. 243, 287–335.

Qiang, Y.W., Yao, L., Tosato, G., Rudikoff, S., 2004. Insulin-like growth factor I induces migration and invasion of human multiple myeloma cells. Blood 103, 301–308.

Rios, H., Koushik, S.V., Wang, H., Wang, J., Zhou, H.M., Lindsley, A., Rogers, R., Chen, Z., Maeda, M., Kruzynska-Frejtag, A., Feng, J.Q., Conway, S.J., 2005. periostin null mice exhibit dwarfism, incisor enamel defects, and an early-onset periodontal disease-like phenotype. Mol. Cell Biol. 25, 11131–11144.

Sanford, L.P., Ormsby, I., Gittenberger-de Groot, A.C., Sariola, H., Friedman, R., Boivin, G.P., Cardell, E.L., Doetschman, T., 1997. TGFbeta2 knockout mice have multiple developmental defects that are non-overlapping with other TGFbeta knockout phenotypes. Development 124, 2659–2670.

Scaffidi, A.K., Moodley, Y.P., Weichselbaum, M., Thompson, P.J., Knight, D.A., 2001. Regulation of human lung fibroblast phenotype and function by vitronectin and vitronectin integrins. J. Cell Sci. 114, 3507–3516.

Schroeder, J.A., Jackson, L.F., Lee, D.C., Camenisch, T.D., 2003. Form and function of developing heart valves: coordination by extracellular matrix and growth factor signaling. J. Mol. Med. 81, 392–403.

Shao, R., Bao, S., Bai, X., Blanchette, C., Anderson, R.M., Dang, T., Gishizky, M.L., Marks, J.R., Wang, X.F., 2004. Acquired expression of periostin by human breast cancers promotes tumor angiogenesis through up-regulation of vascular endothelial growth factor receptor 2 expression. Mol. Cell Biol. 24, 3992–4003.

Shreiber, D.I., Enever, P.A., Tranquillo, R.T., 2001. Effects of pdgf-bb on rat dermal fibroblast behavior in mechanically stressed and unstressed collagen and fibrin gels. Exp. Cell Res. 266, 155–166.

Sugi, Y., Yamamura, H., Okagawa, H., Markwald, R.R., 2004. Bone morphogenetic protein-2 can mediate myocardial regulation of atrioventricular cushion mesenchymal cell formation in mice. Dev. Biol. 269, 505–518.

Taliana, L., Evans, M.D., Dimitrijevich, S.D., Steele, J.G., 2000. Vitronectin or fibronectin is required for corneal fibroblast-seeded collagen gel contraction. Invest. Ophthalmol. Visual Sci. 41, 103–109.

Walsh, E.C., Stainier, D.Y., 2001. UDP-glucose dehydrogenase required for cardiac valve formation in zebrafish. Science 293, 1670–1673.

Yamagishi, T., Nakajima, Y., Miyazono, K., Nakamura, H., 1999. Bone morphogenetic protein-2 acts synergistically with transforming growth factor-beta3 during endothelial–mesenchymal transformation in the developing chick heart. J. Cell. Physiol. 180, 35–45.

Yan, W., Shao, R., 2006. Transduction of a mesenchyme-specific gene periostin into 293T cells induces cell invasive activity through epithelial–mesenchymal transformation. J. Biol. Chem.